Regularized Inversion Method for Frequency-Domain Recovery of the Full Synthetic Aperture Dataset From Focused Transmissions

Rehman Ali
Department of Electrical Engineering
Stanford University
Stanford, CA
rali8@stanford.edu

Jeremy J. Dahl
Department of Radiology
Stanford School of Medicine
Stanford, CA
jjdahl@stanford.edu

Nick Bottenus
Department of Biomedical Engineering
Duke University
Durham, NC
nick.bottenus@duke.edu

***Abstract*—Accurate recovery of the full-synthetic aperture (FSA) dataset from focused transmissions can enable synthetic transmit focusing without the drawbacks of single-element and virtual-element transmissions and enable a wide array of imaging techniques that require the FSA dataset. Recovery of the FSA dataset has previously been performed using an adjoint-based method on a steered transmit sequence for phased-arrays. We present a regularized inversion method for FSA dataset recovery that allows a wider variety of aperture specifications and is intended to perform more accurately in walking aperture sequences. The goal of this method is to improve FSA dataset accuracy and achievable image quality.**

***Index Terms*—Frequency Domain Beamforming, Synthetic Aperture Reconstruction, Regularized Inversion**

I. Introduction

Most commercial ultrasound scanners directly use the backscattered echoes from focused transmit beams to form ultrasound images. Dynamic-receive focusing is often used to form a single A-line from each transmit beam. In this case, resolution becomes limited to only receive focusing away from the transmit focus. Virtual source synthetic aperture can be used to improve transmit focusing by using parallel receive lines for each transmit beam [1]. However, the degree of achievable improvement in transmit focusing is limited to the number of receive lines and the angular coverage of transmit beams through a desired focal point. The performance of a number of imaging applications such as coherence imaging [2], phase-aberration correction [3], and sound speed estimation [4] depend on transmit focusing.

Since the full-synthetic aperture (FSA) dataset consists of receive channel data from individual transmit elements, it can be used to produce transmit focusing everywhere in the ultrasound image [5]. Recently, a method was proposed for reconstructing the FSA dataset from focused transmissions by summing transmit beam data that has been delayed to align at each individual transmit element [6]. This method was tested on a sequence of steered transmit beams from a phased-array and was shown to yield the same imaging resolution as the full-synthetic aperture dataset. One goal of this paper is to examine the performance and limitations of this approach when applied to a walking aperture transmit sequence.

We propose a new method for reconstructing the FSA dataset from a set of focused transmit beams. This method first consists of a formulating a new frequency-domain transmit encoding matrix that incorporates both delay and apodization when relating individual transmit elements to each transmit beam. Second, the method proposes to apply the regularized inverse of this matrix to received, frequency-domain channel data from focused transmits to recover the FSA dataset at each frequency. The approach presented in [6] is equivalent to applying a conjugate transpose, or adjoint, instead of a regularized inverse, of the same transmit encoding matrix at each frequency. The goal of this paper is to demonstrate improvements in reconstruction of the FSA dataset using a regularized inversion approach.

II. Theory

A. Forward Model for Transmit Beamforming

If a pulse is transmitted from element $T \in [1, ..., N_{elem}]$, then $u_{TR}(t)$ is the channel data at receive element $R \in [1, ..., N_{elem}]$ due to transmit element T. Indexed over all transmit and receive element pairs, $u_{TR}(t)$ is referred to as the full synthetic aperture dataset. If delay τ_{nT} and apodization w_{nT} are applied to each transmit element T to obtain transmit beam $n \in [1, ..., N_{beams}]$, then $s_{nR}(t)$, the received channel data for transmit beam n as a function of receive channel R and time t, can be written as

$$s_{nR}(t) = \sum_{T=1}^{N_{elem}} w_{nT} u_{TR}(t - \tau_{nT}). \tag{1}$$

In the frequency domain, this delay-and-sum is equivalent to

$$S_{nR}(f) = \sum_{T=1}^{N_{elem}} A_{nT}(f) U_{TR}(f) \tag{2}$$

where $A_{nT}(f) = w_{nT} e^{-j2\pi f \tau_{nT}}$. In matrix form, this can be written as

$$\boldsymbol{S}_R(f) = \boldsymbol{A}(f) \boldsymbol{U}_R(f) \tag{3}$$

Authorized licensed use limited to: UNIVERSITY OF ROCHESTER. Downloaded on September 12,2026 at 03:31:21 UTC from IEEE Xplore. Restrictions apply.

where $\boldsymbol{U}_R(f) \in \mathbb{C}^{N_{elem}}$, $\boldsymbol{A}(f) \in \mathbb{C}^{N_{beams} \times N_{elem}}$, and $\boldsymbol{S}_R(f) \in \mathbb{C}^{N_{beams}}$.

B. Full-Synthetic Aperture Recovery by Model Inversion

The goal of FSA dataset reconstruction is to obtain an estimate $\hat{\boldsymbol{U}}_R(f)$ of $\boldsymbol{U}_R(f)$ from $\boldsymbol{S}_R(f)$ at each frequency f. This can be accomplished by a pseudoinverse $\boldsymbol{A}^\dagger(f)$ for $\boldsymbol{A}(f)$, and applying it to $\boldsymbol{S}_R(f)$ at each frequency f.

$$\hat{\boldsymbol{U}}_R(f) = \boldsymbol{A}^\dagger(f)\boldsymbol{S}_R(f) = [\boldsymbol{A}^\dagger(f)\boldsymbol{A}(f)]\boldsymbol{U}_R(f) \qquad (4)$$

Ideally $\boldsymbol{A}^\dagger(f)\boldsymbol{A}(f)$ would equal the identity matrix and FSA recovery would be perfect. This work considers two potential pseudoinverses $\boldsymbol{A}^\dagger(f)$.

1) Adjoint (Conjugate Transpose):

$$\boldsymbol{A}^\dagger(f) = \boldsymbol{A}^*(f) \qquad (5)$$

Application of this pseudoinverse is equivalent to the following delay-and-sum operation in the time-domain:

$$\hat{u}_{TR}(t) = \sum_{n=1}^{N_{beams}} w_{nT} s_{nR}(t + \tau_{nT}). \qquad (6)$$

This approach, introduced in [6], essentially delays each transmit beam to align at each transmit element, and the result is coherently summed over transmit beams to recover an estimate of receive channel data due to each transmit element.

2) Tikhonov-Regularized Inversion:

$$\boldsymbol{A}^\dagger(f) = [\boldsymbol{A}^*(f)\boldsymbol{A}(f) + (\gamma\sigma_{max}(f))^2\boldsymbol{I}]^{-1}\boldsymbol{A}^*(f) \qquad (7)$$

where $\sigma_{max}(f)$ is the maximum singular value of $\boldsymbol{A}(f)$, and γ is a regularization parameter that penalizes $\left\|\hat{\boldsymbol{U}}_R(f)\right\|_2$. The purpose of this regularization to suppress the amplification of noise due to inversion of small singular values in $\boldsymbol{A}(f)$, especially at low frequency f. Because of the highly variable effect that this pseudoinverse has on each transmit element at each frequency, there is no obvious time-domain equivalent for this approach.

III. Methods

A. Transmit Simulation

The complete FSA dataset was simulated in Field II for a medium of random diffuse point scatterers whose reflectivities were modified to simulate an anechoic lesion and two hyperechoic lesions. Simulation parameters such as the transducer configuration and transmit pulse are described in Table I.

Focused transmit beams were simulated by combining receive channel data from each transmit element according to equation (1). Delays for the walking aperture transmit sequence were calculated as

$$\tau_{nT} = \frac{1}{c}\left\{\sqrt{x_n^2 + z_n^2} - \sqrt{(x_T - x_n)^2 + z_n^2}\right\} \qquad (8)$$

where (x_n, z_n) is the transmit focus, $(x_n, 0)$ is the beam origin, and $(x_T, 0)$ are the coordinates of the transmit element T. Table II describes the walking aperture transmit sequence simulated using the FSA dataset from Field II and equations (1) and (8).

TABLE I
FIELD II SIMULATION SETTINGS

Parameter	Value	Units
Array Geometry	Linear	-
Number of Elements	96	elements
Element Pitch	0.154	mm
Center Frequency	5	MHz
Fractional Bandwidth	0.7	-
Speed of Sound	1540	m/s
Sampling Frequency	100	MHz

TABLE II
WALKING-APERTURE TRANSMIT SEQUENCE IN FIELD II

Parameter	Value	Units
Focal Depth	30	mm
Transmit Angle	0	degrees
Beam Origins	[-3.65, 3.65]	mm
Beam Origin Step	0.05	mm
Aperture Width (Around Beam Origin)	8	mm
Transmit Apodization	Rectangular	-

B. Measurement of Time-Domain Reconstruction Error

In order to evaluate the accuracy of FSA dataset reconstruction using each pseudoinverse (5) and (7), the time-domain error was measured relative to the true FSA dataset directly simulated in Field II.

The amplitude of the time domain signal decreases with time due to the geometrical spreading of the acoustic wave. Time-gain compensation is applied to both the recovered and true FSA datasets in order to adjust for this geometric spreading prior to measuring the relative time domain reconstruction error. The relative time-domain reconstruction error after time-gain compensation is given as

$$\epsilon_{rel} = \frac{\int_{-\infty}^{\infty}(t\hat{u}_{TR}(t) - tu_{TR}(t))^2 dt}{\int_{-\infty}^{\infty}(tu_{TR}(t))^2 dt} \times 100\%. \qquad (9)$$

For the adjoint pseudoinverse (5), $\hat{u}_{TR}(t)$ is scaled to minimize ϵ_{rel} because the scaling of the adjoint is arbitrary.

C. Full-Synthetic Aperture Image Reconstructions

To demonstrate the practical impact of FSA dataset recovery on image reconstruction, the FSA image reconstructed from the recovered datasets was compared to the FSA image reconstructed from the true FSA dataset. For experimental demonstration, a walking aperture sequence summarized in Table III was implemented on the L12-3v ultrasound probe and data was acquired on a CIRS 040GSE phantom. FSA datasets were recovered for each choice of pseudoinverse, and corresponding FSA images were reconstructed. Resolution, speckle structure, and artifacts in the resulting images were compared.

Authorized licensed use limited to: UNIVERSITY OF ROCHESTER. Downloaded on September 12,2026 at 03:31:21 UTC from IEEE Xplore. Restrictions apply.

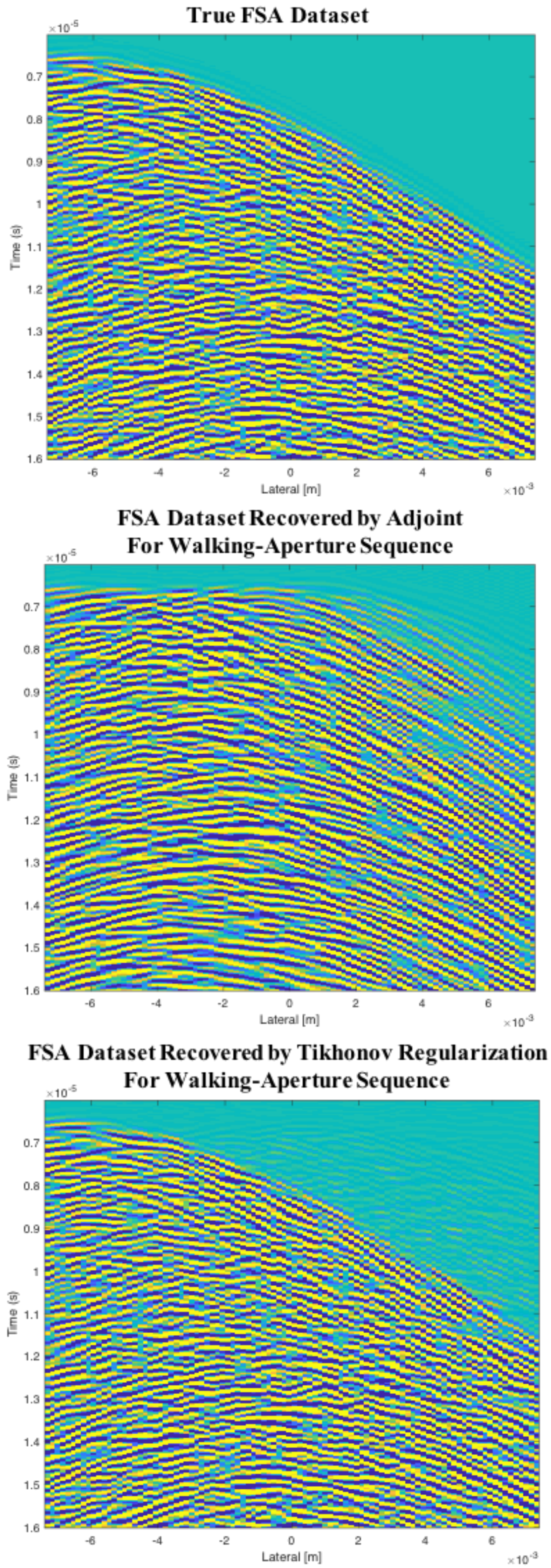

Fig. 1. Reconstruction of the FSA dataset using the adjoint and Tikhonov regularization to decode the walking-aperture transmit sequence in Table II. Reconstruction errors are 103.83% and 11.32% when using the adjoint and Tikhonov regularization ($\gamma = 0.01$), respectively. Images show the time-gain compensated received channel data vs time for the first transmit element on the array.

TABLE III
WALKING-APERTURE TRANSMIT SEQUENCE ON VERASONICS L12-3V

Parameter	Value	Units
Transmit Frequency	7.8130	MHz
Focal Depth	13.8	mm
Transmit Angle	0	degrees
Beam Origins	[-19.1, 19.1]	mm
Beam Origin Step	0.2	mm
Aperture Width (Around Beam Origin)	25.2	mm
Transmit Apodization	Rectangular	-

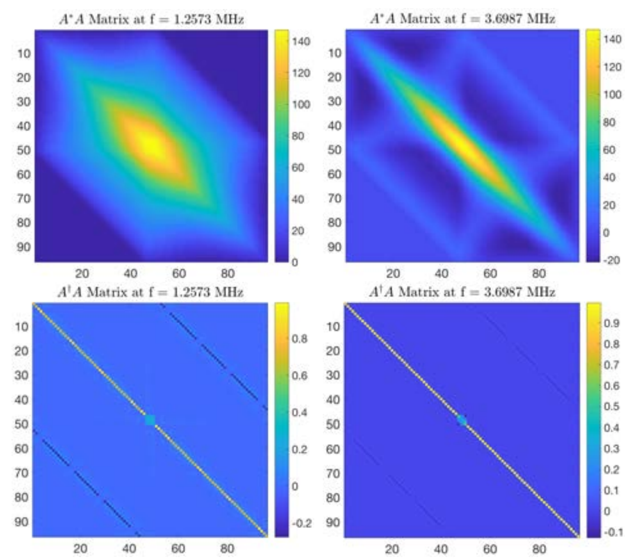

Fig. 2. Comparison of $\boldsymbol{A}^*(f)\boldsymbol{A}(f)$ to $\boldsymbol{A}^\dagger(f)\boldsymbol{A}(f)$ based on Tikhonov regularization ($\gamma = 0.01$) for walking-aperture transmit sequence in Table II.

IV. RESULTS

A. Comparison of Pseudoinverses for FSA Dataset Recovery

Figure 1 compares a segment of the true FSA dataset to the recovered datasets from each pseudoinverse. Dataset reconstruction error was much greater when the adjoint ($\epsilon_{rel} = 103.83\%$) was used as the pseudoinverse. This is because $\boldsymbol{A}^*(f)\boldsymbol{A}(f)$ does not yield a good approximation of the identity matrix in the walking aperture case. Examples of $\boldsymbol{A}^*(f)\boldsymbol{A}(f)$ at two different frequencies f are shown in the top row of Figure 2. At each frequency, the diagonal of $\boldsymbol{A}^*(f)\boldsymbol{A}(f)$ reveals that each transmit element experiences a different gain due to the adjoint-based reconstruction. Furthermore, at low frequency f, the off-diagonal terms of $\boldsymbol{A}^*(f)\boldsymbol{A}(f)$ show that there is significant crosstalk between transmit elements. These deviations in $\boldsymbol{A}^*(f)\boldsymbol{A}(f)$ from the identity matrix at each frequency explains the time-domain reconstruction errors seen in the recovered dataset when using the adjoint. However, the bottom row of Figure 2 shows that Tikhonov regularization yields an $\boldsymbol{A}^\dagger(f)\boldsymbol{A}(f)$ matrix that more reasonably approximates the identity; as a result dataset reconstruction error ϵ_{rel} was only 11.32% when Tikhonov regularization was used instead.

Authorized licensed use limited to: UNIVERSITY OF ROCHESTER. Downloaded on September 12,2026 at 03:31:21 UTC from IEEE Xplore. Restrictions apply.

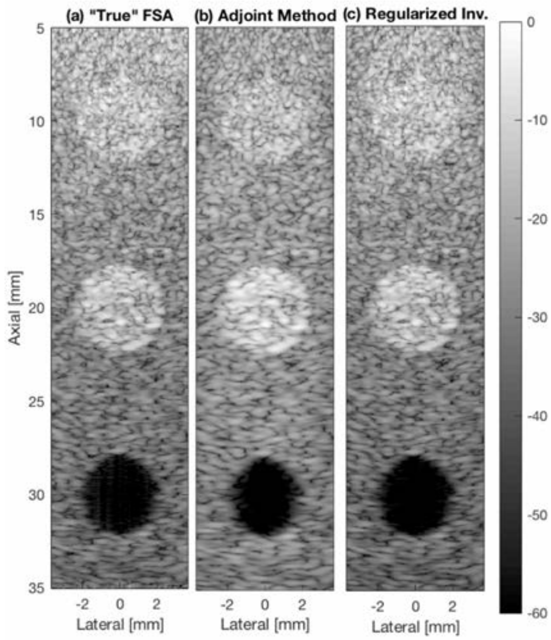

Fig. 3. FSA image reconstruction based on datasets recovered using the adjoint and the Tikhonov-regularized inverse to decode the walking aperture transmit sequence described in Table II. Simulations show that both the speckle structure and resolution of the true FSA image (a) are better retained in the proposed method (c) compared to the adjoint-based method (b). At 33 mm depth, error in resolution (-6 dB width) was 28.7% and <0.1% for adjoint-based (b) and proposed (c) methods, respectively. The normalized RMS error in image reconstruction was 50% for adjoint-based method (b) and 7% for the proposed method (c).

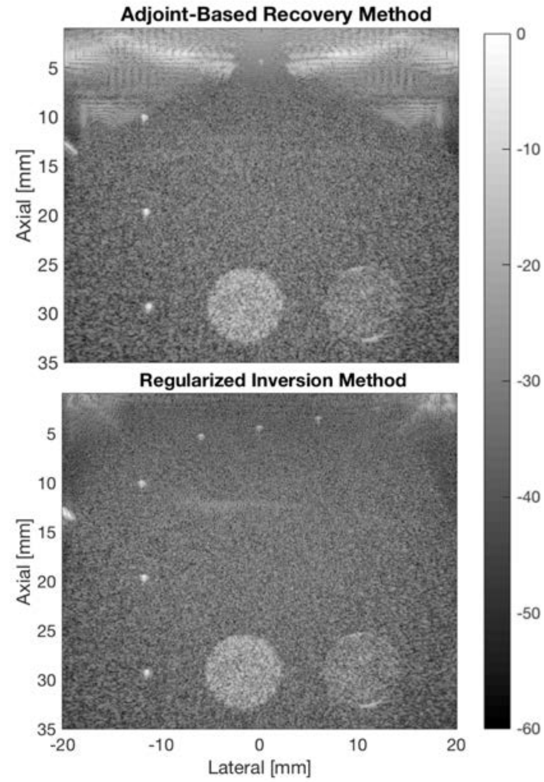

Fig. 4. FSA image reconstruction based on datasets recovered using the adjoint and the Tikhonov-regularized inverse to decode the walking aperture transmit data (sequence described in Table III) captured using an L12-3v linear array with a Verasonics Vantage 256 scanner on a CIRS 040GSE phantom.

B. FSA Image Reconstruction Based on Recovered Datasets

Figures 3 and 4 shows FSA image reconstruction using datasets recovered from walking aperture transmit sequences based on Field II simulation and phantom experiments, respectively. The results of Field II simulation shows that the adjoint decoding is unable to recover the imaging resolution achievable using true FSA dataset. The speckle structure of the FSA image reconstructed based on the dataset recovered using Tikhonov regularization better matches the FSA image reconstructed using the true FSA dataset. Phantom experiments show that Tikhonov regularization accomplishes a decoding that improves the visibility of point targets in the near field that were not previously visible using the adjoint decoding.

V. Conclusions

For walking-aperture transmit sequences, it appears that the adjoint-based recovery method does not accurately decode the receive channel data from each individual transmit element. However, Tikhonov regularization yields a highly accurate decoding that recovers the FSA dataset with observable improvements in image reconstruction. Ultimately, these decoding schemes fundamentally impact various imaging applications that depend on recovering the FSA dataset. Future work should examine the k-space response of these encoding-and-decoding schemes to completely characterize their ability to recover the FSA dataset.

Acknowledgment

Rehman Ali would like to thank the National Defense Science and Engineering Graduate (NDSEG) Fellowship for funding his graduate studies and research work. This work was also funded by NIH R01-EB017711 from the National Institute of Biomedical Imaging and Bioengineering and the Duke-Coulter Translational Partnership Grant.

References

[1] M.-H. Bae and M.-K. Jeong, "A study of synthetic-aperture imaging with virtual source elements in b-mode ultrasound imaging systems," *IEEE transactions on ultrasonics, ferroelectrics, and frequency control*, vol. 47, no. 6, pp. 1510–1519, 2000.

[2] N. Bottenus, B. C. Byram, J. J. Dahl, and G. E. Trahey, "Synthetic aperture focusing for short-lag spatial coherence imaging," *IEEE transactions on ultrasonics, ferroelectrics, and frequency control*, vol. 60, no. 9, pp. 1816–1826, 2013.

[3] M. Karaman, H. S. Bilge, and M. O'Donnell, "Adaptive multi-element synthetic aperture imaging with motion and phase aberration correction," *IEEE transactions on ultrasonics, ferroelectrics, and frequency control*, vol. 45, no. 4, pp. 1077–1087, 1998.

[4] M. Jakovljevic, S. Hsieh, R. Ali, G. Chau Loo Kung, D. Hyun, and J. J. Dahl, "Local speed of sound estimation in tissue using pulse-echo ultrasound: Model-based approach," *The Journal of the Acoustical Society of America*, vol. 144, no. 1, pp. 254–266, 2018.

[5] J. A. Jensen, S. I. Nikolov, K. L. Gammelmark, and M. H. Pedersen, "Synthetic aperture ultrasound imaging," *Ultrasonics*, vol. 44, pp. e5–e15, 2006.

[6] N. Bottenus, "Recovery of the complete data set from focused transmit beams," *IEEE transactions on ultrasonics, ferroelectrics, and frequency control*, vol. 65, no. 1, pp. 30–38, 2018.

Authorized licensed use limited to: UNIVERSITY OF ROCHESTER. Downloaded on September 12,2026 at 03:31:21 UTC from IEEE Xplore. Restrictions apply.